UCRL-11850

University of California

Ernest O. Lawrence Radiation Laboratory

THE THERMOCHEMISTRY OF DI- AND TRI-VALENT EUROPIUM

Berkeley, California

DISCLAIMER

UCRL-11850

UNIVERSITY OF CALIFORNIA

Lawrence Radiation Laboratory
Berkeley, California

AEC Contract No. W-7405-eng-48

THE THERMOCHEMISTRY OF DI- AND TRI-VALENT EUROPIUM

John L. Burnett

(Ph.D. Thesis)

December 18, 1964

THE THERMOCHEMISTRY OF DI- AND TRI-VALENT EUROPIUM

Contents

THE THERMOCHEMISTRY OF DI- AND TRI-VALENT EUROPIUM

John L. Burnett

Lawrence Radiation Laboratory
University of California
Berkeley, California

December 18, 1964

ABSTRACT

The construction and operation of a semi-adiabatic microcalorimeter are discussed in detail. The heat of solution of europium metal in 0.1 N HCl has been measured and is -164.6 ± 1.0 Kcal/mole. This value is combined with available thermochemical data to calculate:

$$\Delta H^{\circ}_{f Eu^{+3}_{(aq)}} = -130.4 \pm 1.0 \text{ Kcal/mole.}$$

The preparation and properties of europium monoxide, prepared by reacting the metal with the sesquioxide at high temperature are described. It has been characterized by:

1. Crystal structure: fcc, NaCl type.
2. Lattice parameter: 5.143 ± 0.001 Å.
3. Stoichiometry: O/Eu = 1.021 ± 0.001
4. Thermodynamics: $\Delta H_{soln.} = -87.8 \pm 1.7$ Kcal/mole
   yielding $\Delta H^{\circ}_{f EuO_{(c)}} = -145.1 \pm 2.2$ Kcal/mole.

These heats of formation are combined with other thermochemical data to calculate the heat of formation of $Eu^{+2}_{(aq)}$: -114.3 Kcal/mole; the $Eu\text{-}Eu^{+2}_{(aq)}$ potential: +2.51 volts; and the free energy of disproportionation of EuO: +39.9 Kcal. The $S^{\circ}_{Eu^{+3}_{(aq)}}$ is estimated to be -37.1 e.u.

I. INTRODUCTION

In recent years, an increasing amount of thermodynamic information on the rare earths and their compounds has been published. While the picture is by no means complete, heats of formation are known for most of the oxides, and some of the trihalides and tripositive aqueous ions. Entropy data are available for many of the oxides and metals.

Until very recently, there have been no experimental thermochemical data on europium. Published values are either estimates or interpolations from plots of available data on the other rare earths. However, europium metal differs markedly from most of the other rare earths in its physical properties, and since the metal is the reference state for the thermochemical measurements, it seems reasonable to expect that the heats and free energies of formation of europium ions and compounds would show marked deviations from the corresponding values for those other rare earths.

In the following work the experimental procedure followed in the determination of the heats of formation of $Eu^{+3}_{(aq)}$ and $EuO_{(c)}$ is presented. The results are combined with available thermodynamic data to calculate the heat for formation of $EuCl_{3(c)}$, $Eu^{+2}_{(aq)}$, the $Eu\text{-}Eu^{+2}$ aqueous potential, and the free energy of disproportionation of $EuO_{(c)}$. $EuO_{(c)}$ is also characterized as to lattice parameter and stoichiometry. The results are discussed in their comparisons with other rare earths and the alkaline earths.

II. MICROCALORIMETER

A. Construction

The microcalorimeter used for all heat measurements is a semi-adiabatic instrument with a vacuum jacket and water bath thermostated at 25°C. The heat capacity is approximately nine calories per degree and the temperature sensitivity about 1×10^{-5} degree. A general view of the instrument is shown in Fig. 1.

A sectional drawing of the submarine chamber with the calorimeter unit in place is shown in Fig. 2.[1] The calorimeter reaction chamber, M, is suspended inside the stainless steel submarine chamber, O, by means of a hollow lucite hanger vacuum sealed at both ends with Neoprene O-rings. This hanger is about $1\frac{1}{2}$ inches long with a narrow neck about $\frac{1}{2}$ inch long, 0.100 inch outside diameter, and 0.065 inch inside diameter. Halfway up the neck is a lucite guide 0.125 inch long with a 0.042 inch coaxial hole. The stirring shaft, I, passes through this hanger and the guide minimizes friction and eccentricity in the stirring action. The stirring shaft is a quartz rod about 0.042 inch in diameter which is clamped at the upper end by means of a Bakelite collet in the stirring chuck. The chuck is fitted with a spring loaded screw-in-slot arrangement, D, to permit depression of the shaft a certain distance to break the sample bulb which is attached to the lower end of the shaft. Stirring speed is about 300 revolutions per minute through a flexible shaft to the stirring chuck. A platinum resistance thermometer and calibrating heater connecting leads, K, L, are conducted through holes in the submarine frame to copper binding posts, A, for the thermometer and a 4-pronged plug, B, mounted in a plastic block, C, for the heater. The stainless steel submarine chamber is about three inches long by about 1-3/4 inches in diameter and is screwed onto the frame against a

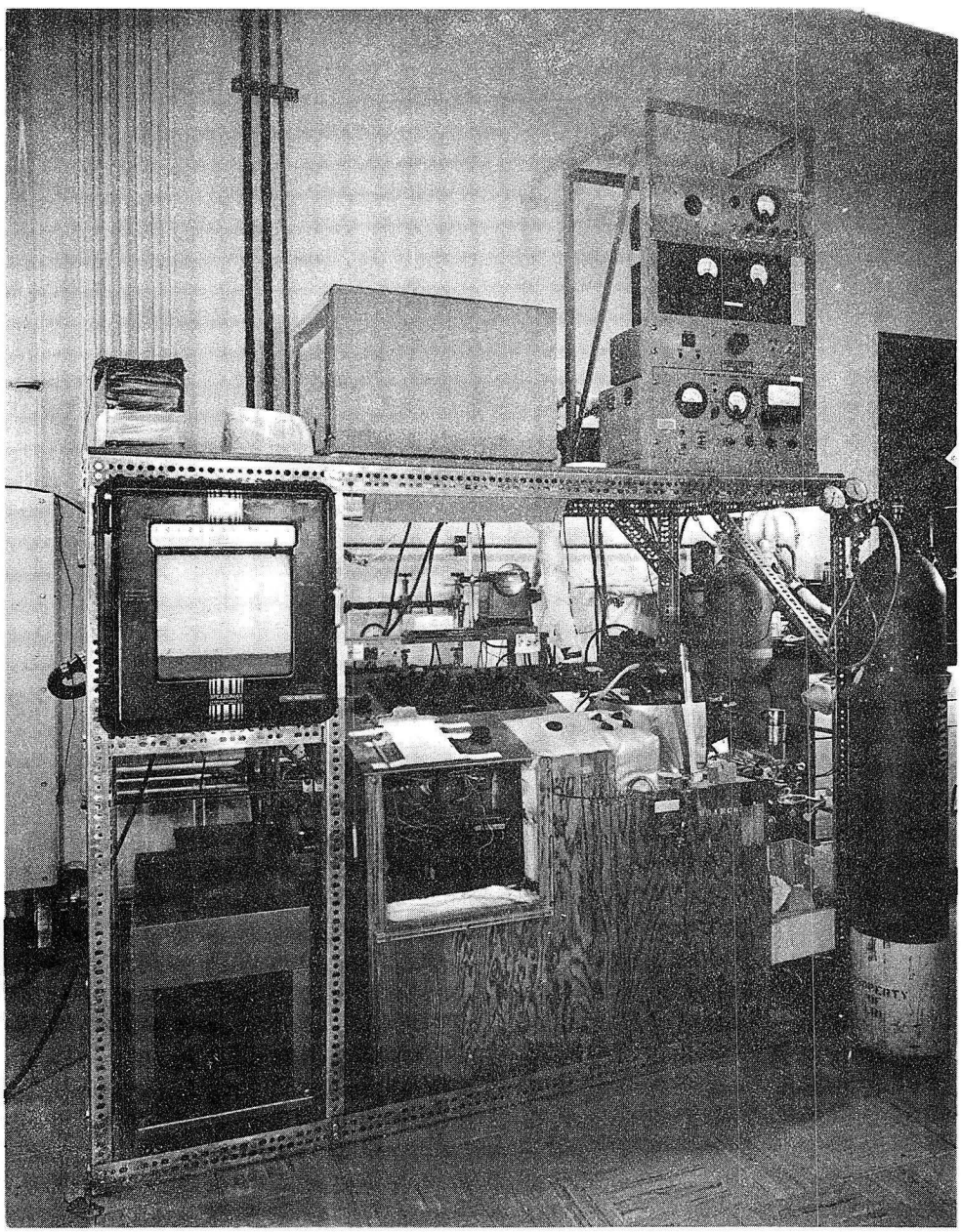

ZN-4596

Fig. 1. General view of microcalorimeter.

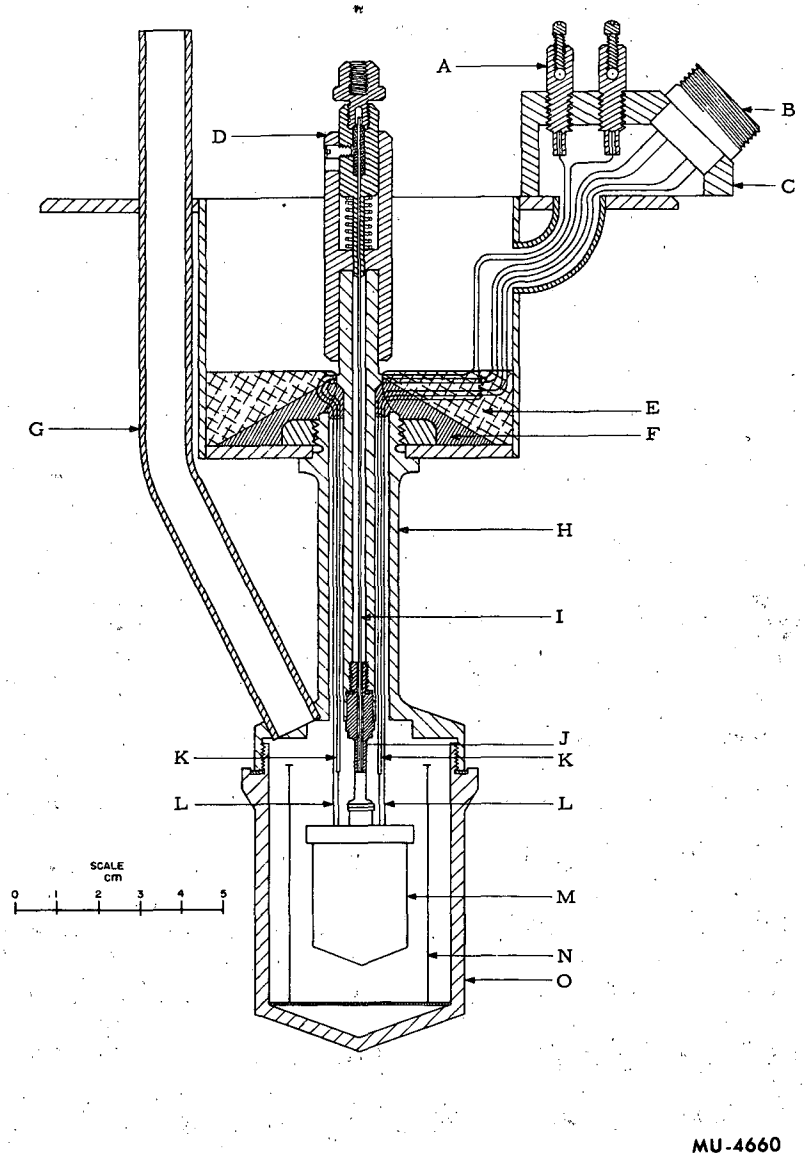

Fig. 2. Microcalorimeter cross section.

greased Neoprene gasket for a vacuum seal. A radiation shield, M, consisting of two concentric tantalum cylinders is placed inside the submarine chamber to minimize radiation heat transfer. This space is evacuated by means of a mercury diffusion pump and liquid nitrogen trap backed up by a Welch Duo-seal fore pump. The usual vacuum is 1×10^{-5} to 5×10^{-6} mm Hg. The thermal leakage modulus, k, as defined by the expression:

$$k = -\frac{1}{\theta}\frac{d\theta}{dt}$$

where θ is the difference between the temperature of the calorimeter and the temperature when it is in equilibrium with the thermostat and t is the time, is about 5×10^{-3} min.$^{-1}$. The principle heat leaks now are along the hanger, stirring shaft, and electrical leads.

The calorimeter unit is shown in Fig. 3.[1] The tantalum reaction vessel, H, has about a 9 ml. capacity. The cap, F, the four thermometer and heater conduits, G, and the spool and sleeve, I,J, are also tantalum with gold soldered joints where the conduits join the spool and cap. This end of the stirring shaft, B, holds the 4-bladed platinum propeller, K, and the sample bulb, L, both sealed onto the shaft with Apiezon W wax. Depressing the shaft from the stirring chuck above crushes the bulb against the anvil, M, admitting the sample to the solution.

The construction and packaging of the thermosensitive element and calibrating heater is a delicate operation. The thermometer is one mil pure Pt wire and the heater is either #44 Manganin or #40 Karma wire. These are wound non-inductively on a mica strip 1.45 cm. X 4.50 cm. X 1-2 mil thick which has been notched along the edges to hold the wires in place. The Pt is wound on one end and the heater on the other. This strip is then sandwiched between two more mica strips and the combination wrapped around the tantalum spool and held in place with

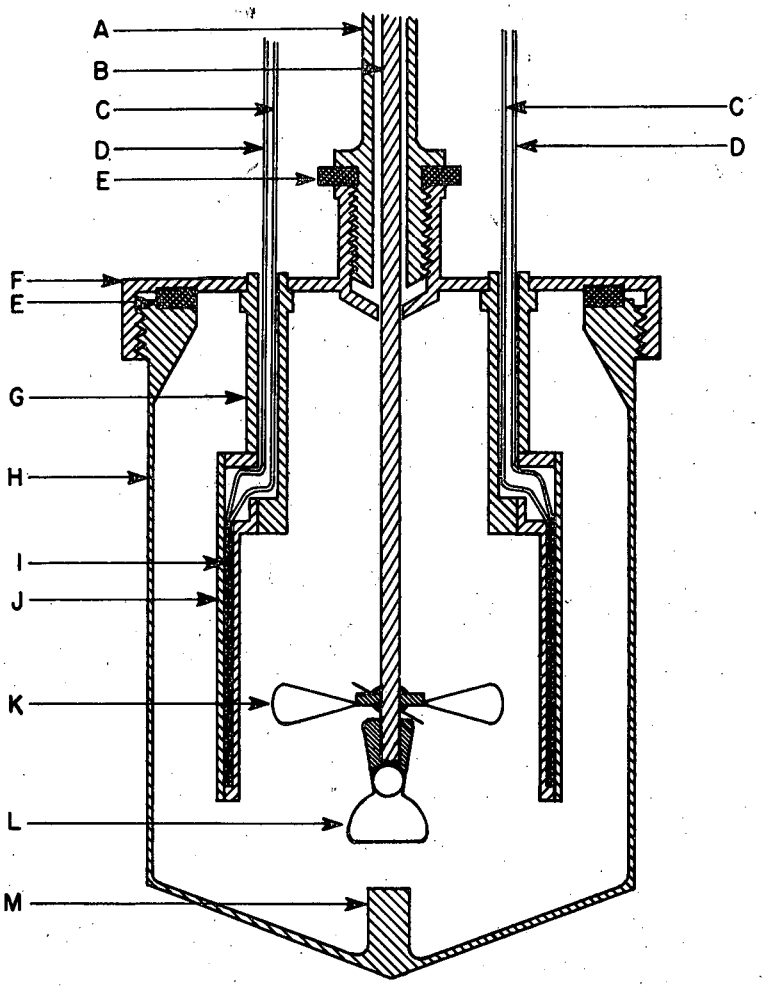

Fig. 3. Microcalorimeter cross section of reaction.

three lengths of 5 mil tantalum wire. The assembly must now be annealed to relieve strains in the wires. Earlier, spools made in this way had only about 5000 ohms resistance between the thermometer and heater and thermometer and body after annealing, while this resistance should be thousands of megohms. It was found that the annealing process was responsible for the lower resistance, apparently as the result of volatilization and condensation of a conducting film of tantalum oxide. The parts had been cleaned in dilute acid, water, and alcohol; but it was now thought that a much more thorough cleaning was required. So all tantalum parts were heated in a 8 M HNO_3-2 M HF solution at 100°C for about 5 minutes; the mica and heater and thermometer wires were carefully cleaned of all contaminants; and then all parts handled with rubber gloves thereafter. Annealing is done at about 600°C under high vacuum for about 18 hours. Such spools after annealing have resistances that are thousands of megohms or are unmeasurable.

Since the thermometer is one leg of a Wheatstone bridge, its resistance must be adjusted so that it will balance with the bridge circuit. Accordingly, the Pt wire is trimmed until the desired resistance is obtained.

Fine quartz capillaries serve as insulators in the four conduits and 8-10 mil Au wire is used for the thermometer leads. No solder is required as the Au and Pt are directly welded with a microtorch. The heater leads are #34 Cu wire. In joining the Cu to the Manganin or Karma a solder is usually used, but sometimes a direct weld can be made by melting the Cu. All leads and connections are generously coated with polystyrene Q-dope and arranged in the channel in the spool just above the mica. The sleeve is slipped on and sealed in place with epoxy resin.

After drying and curing of the epoxy, final sealing of the spool-sleeve seam is done with Apiezon W wax dissolved in toluene and painted on. The quartz insulators are sealed at the top of the cap with Q-dope or epoxy resin.

As was previously indicated, the thermometer circuit is a Wheatstone bridge as shown in Fig. 4. The decade, D, is in a steel box to provide proper shielding. Extending from the bottom of this box into the thermostat is an oil filled iron pipe containing R_1, R_2, R_3, and R_4. A six volt storage battery cut and wired to give two volts provides a source of very constant current to the bridge which draws about 36 milliamperes. The low pass filter is designed to attenuate a. c. frequencies much greater than one cps. The potential divider, R_{10}, R_{11}, may be used to reduce the sensitivity by about a factor of ten, and under these conditions the entire time-temperature curve can be recorded graphically. Thus accurate corrections for thermal leakage can be computed from the curve. This will be discussed in more detail later.

The d. c. breaker amplifier is a Beckman Model 14 with an input impedance of 50 ohms. The recorder is a Leeds and Northrup Speedomax Type G dual range, dual speed, self-standardizing model. Erratic behavior of the original system was traced to temperature sensitivity of the decade box, the breaker amplifier input cable, and the breaker amplifier itself. Therefore the box and cable are wrapped in pads of glass wool insulating material and the amplifier is enclosed in a styrafoam box and is cooled by a stream of air.

The heater and timer circuit is shown in Fig. 5. The input to the heater circuit is a stabilized 115 volts and the timer input is a standard 60 cps frequency which is divided down to 1 cps. This is

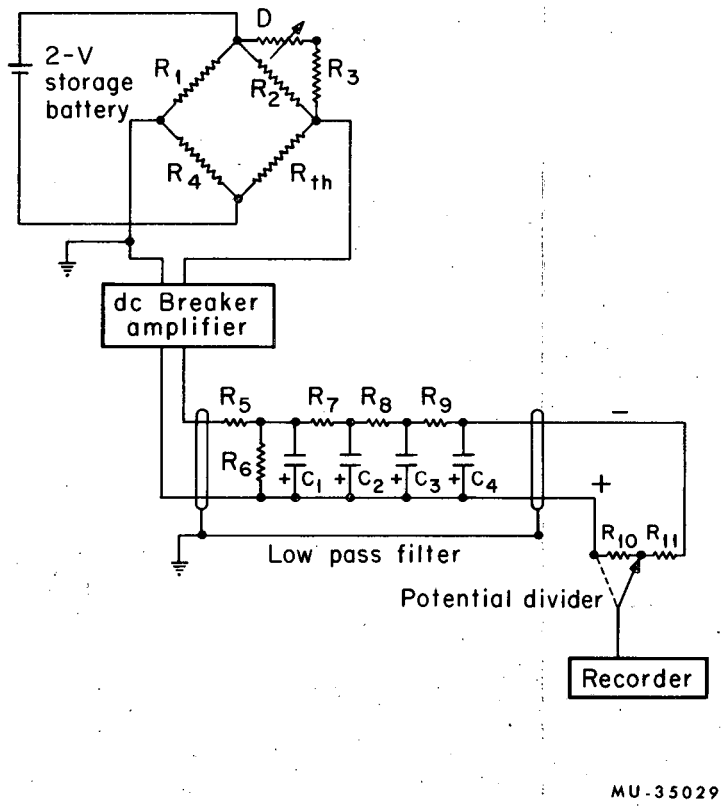

Fig. 4. Thermometer circuit.

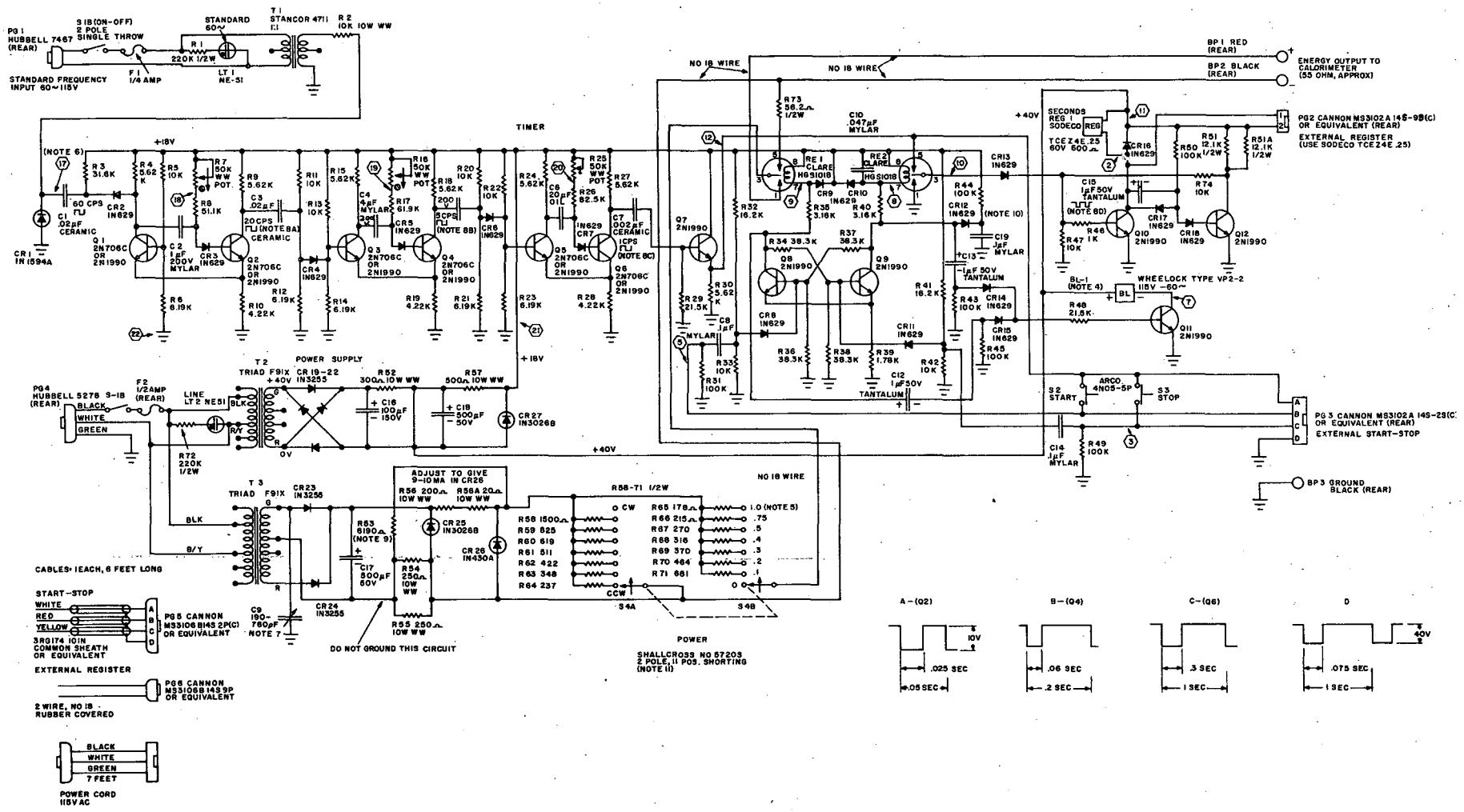

MUB-4967

Fig. 5. Heater and timer circuit.

NOTES FOR FIG.5

1. All resistors are coated metal film types unless otherwise specified. When the wattage is not indicated, 1/8, 1/4, or 1/2 watt may be used, but 1/2 watt is preferred when space permits.

2. Overall operation of the divider network can be checked by putting on "0" and pressing "start" button. It is necessary to hold the start button down for a time not exceeding 1 sec. The register then records the elapsed time in seconds between sounds of the bell, which can be compared with any standard clock. The "stop" button turns off the counter at any integral second.

3. The timing error due to delay in operation of RE-1 can be determined by placing the "power" switch on 0.1 and using the "energy output" as a gate to control a timer operating at a frequency of 10kc or higher. The net error should not be more than a few milliseconds, and is reproducible.

4. This bell is polarized and the polarity must be determined so that the gong sounds when current is applied.

5. These numbers indicate the fraction of maximum power being applied. The "power" switch, S-4, should be labled with these numbers.

6. Numbers in hexagons refer to pin numbers on Plug-In board.

7. Adjust C-9 to minimize hum between floating "Energy Output" negative lead and ground.

8. R-53 is adjusted so that variation in line voltage has minimum affect on "Energy Output" voltage.

9. C-19, CR-12, and R-44 serve only to insure that when the one switch is turned on, the flip-flop Q8-Q9 always comes on in the "stop" position.

10. After turning on "power" switch, the 8.4 volt regulated supply for the "Energy Output" is within 0.1% of the final value in 15 sec., within 0.05% in 90 sec., and within 0.01% in 2 hrs.

11. Q-1, Q-2, Q-3, Q-4, Q-5, and Q-6 (2N706C) may be replaced by 2N1990's.

coupled to the heater circuit output and through on and off switches that start and stop the heater power on the full second. A bell sounds when the heating starts and when it stops; a register records the number of seconds. The accuracy of the timing and stability of the output are good to a few hundreths of a percent. A multiple pole switch permits selection of the fraction of maximum power to be applied. These fractions are 0.1, 0.2, 0.3, 0.4, 0.5, 0.75, and 1.0. The current measuring resistor, which is in series with the calorimeter heater, is of the Manganin wire-wound type and is located in an oil bath. It has proved to be stable to a few thousandths of an ohm over a year's time. A Rubicon Type B High Precision Potentiometer and box lamp and scale galvonometer are used to measure the voltage drops across the current measuring resistor and calorimeter heater. Calibration heat inputs are on the order of 0.2 to 0.4 cal. and agree to a few hundreths of a percent.

The sample is contained in a small pyrex bulb of about 50μl capacity and about 40 mg. in weight, with a flat, very thin bottom. Previously, the bulbs were sealed with an Apiezon W coated pyrex bead in the neck, but the gas in the bulb that escapes upon sealing contributed a large uncertainty to the weight of the sample. Now a fine pyrex capillary tube is inserted into the bulb alongside the bead. (See Fig. 6). A ball of Apiezon W wax is placed in the neck on top of the bead and the bulb is sealed as before with a hot wire, except that the capillary permits re-entry of gas to the bulb as the bulb cools. A piece of 3-mil tungsten wire with a small bead of wax is now inserted into the outer end of the capillary and quickly sealed with a fine point hot wire. The resultant weight loss and uncertainty are $3.50 \pm 0.25\mu g$. This uncertainty is usually less than 0.1% of the sample weight. Weighings are done on a Rodder Model E quartz fibre torsion balance sensitive to $\sim 0.05\mu g$.

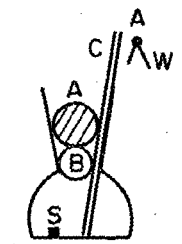

Assembled bulb

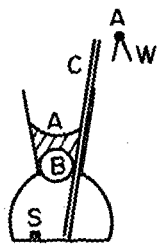

First sealing

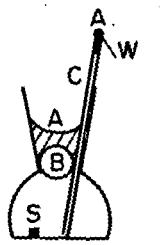

Final sealing

MU-35030

Fig. 6.
A. - Wax
B. - Glass bead
C. - Pyrex capillary
S. - Sample
W. - Wire

B. Operation

Usually, a sample is loaded one day and run the next morning. The thermostat temperature is lowered a few tenths of a degree and the submarine chamber is set in place and connected to the vacuum line. At this point, the temperature of the calorimeter rapidly approaches that of the bath because the vacuum in the chamber is poor. The next morning, however, the vacuum is good and when the thermostat temperature is returned to 25°C the calorimeter temperature lags behind. From four to six calibrating heat inputs are now made which raise the calorimeter temperature nearer the equilibrium point. This point is a few tenths of a degree above the thermostat due to stirring, thermometer current, and friction of the stirring shaft against the hanger.

As this calorimeter is only semiadiabatic, there is a constant drift of the calorimeter temperature toward the equilibrium temperature—the drift rate being determined by the thermal leakage modulus and the temperature difference. This drift is tracked on the recorder. The reaction of interest is initiated at the proper time, such that the heat evolved raises the calorimeter temperature from a point below the equilibrium temperature to a point above. The more nearly equal the corresponding temperature differences are, the smaller the thermal leakage correction. Now several more calibrating heat inputs are made to complete the run. Between each heat input a sensitivity check is made to determine the number of recorder chart divisions per ohm change on the decade.

To check the performance of the calorimeter and the technique of the operator, samples of very pure crystalline magnesium were run in 1.00M HCl solutions and compared with the value obtained by Shomate and Huffman[2] on a much larger scale. The samples were freshly cut and

mechanically cleaned of all oxide, weighed on the previously mentioned torsion balance, and the weight corrected to vacuum. The measured heat evolution was corrected for evaporation of water into the dry hydrogen evolved and into the dry atmosphere in the bulb, and for the heat of breakage of the sample bulb. The latter was determined by breaking several bulbs containing a small amount of water and was found to be about $(6\pm3) \times 10^{-4}$ calories per bulb.

C. Calculation

To exemplify the calculations involved the evaluation of one calibrating heat input and the solution reaction for a magnesium run will be presented.

The amount of heat put into the calorimeter can be represented by the resistance change on the decade required to rebalance the bridge. For this to be strictly true, the position of the track on the chart paper after a heat input must be returned to exactly the same position that it had at the initiation of the heat input. However, since the heat input itself and re-equilibration of the system require a finite length of time, extrapolations of the fore-slope and after-slope to the same time—midpoint of the heating interval—are used. Also, since the decade can be changed only by integral amounts, the two extrapolated points do not usually coincide, but are separated by a certain distance represented by a certain number of chart divisions. This distance can be converted to ohms and fractions thereof by dividing by the sensitivity in divisions per ohm. Thus the decade change required to return the bridge to the same balance point can be calculated.

If, now, the calorimeter heat capacity and the temperature coefficient of resistance of the thermometer are constant in the temperature range of the run, the fractional change of the resistance of the thermometer will be constant for a given amount of heat added, regardless of the initial temperature. Thus, referring to Fig. 4, the fractional change of the resistance in the variable arm of the bridge and the fractional change in the resistance of the thermometer are equal to

$$\text{f.c.} = \frac{\dfrac{500(25{,}000 + R_a)}{500 + 25{,}000 + R_a} - \dfrac{500(25{,}000 + R_f)}{500 + 25{,}000 + R_f}}{\dfrac{500(25{,}000 + R_f)}{500 + 25{,}000 + R_f}}$$

where R_a and R_f are the decade values for the after-slope and fore-slope respectively. Or, more simply:

$$f.c. = \left(\frac{25,000 + R_a}{25,000 + R_f}\right)\left(\frac{25,500 + R_f}{25,500 + R_a}\right) - 1.$$

The amount of heat for a given input can be precisely calculated, so the fractional change per calorie can be calculated. These values are averaged over several heat inputs and the average applied to the fractional change calculated for the heat of reaction of interest.

The example heat input was for 60 seconds at 0.4 maximum power, and gave for the voltage drops across the standard current measuring resistor and the calorimeter heater, 0.84235 v. and 0.54997 v. respectively. Thus we calculate:

$$Q = \frac{I_H^2 R_H t}{4.184}$$

$$= (E_{st})(E_H)\frac{t}{R_{st}\ 4.184}$$

The value of R_{st} is 24.809Ω; thus for this heat input:

$$Q = 0.84235 \times 0.54997 \times \frac{60}{24.809 \times 4.184}$$

$$= 0.26778 \text{ cal.}$$

The decade value for the fore-slope was 2965Ω and for the after-slope was 3128Ω. Both slopes were extrapolated to the midpoint of the heat input. The extrapolation of the after-slope was 4.7 chart divisions down scale from that of the fore-slope which means that the resistance change on the decade, 163Ω, was too large to return the bridge to its former balance point. Sensitivity checks are made at intervals throughout the run, as indicated previously, and are plotted as divisions per ohm vs. average ohms on the decade. The sensitivity for this heat input was 2.564 $\frac{\text{div.}}{\Omega}$. Thus the decade change required to balance the

bridge was:

$$163\Omega - \frac{4.7 \text{ div}}{2.564 \frac{\text{div}}{\Omega}} = 161.17\Omega$$

The after-slope resistance, then, should be 3126.17Ω. The fractional change can then be calculated:

$$\text{f.c.} = \left(\frac{25{,}000 + 3126.17}{25{,}000 + 2965}\right)\left(\frac{25{,}500 + 2965}{25{,}500 + 3126.17}\right) - 1$$

$$= 1.0057632755 \times 0.9943698371 - 1$$

$$= 0.0001006649$$

and the fractional change per calorie is then:

$$\frac{\text{f.c.}}{\text{cal}} = \frac{0.0001006649}{0.26778}$$

$$= 3.75924 \times 10^{-4}$$

Similarly, the fractional change per calorie for the other heat inputs is calculated and the values averaged.

The calculation of the fractional change for the reaction involves correction for the net heat leakage between the calorimeter and the environment. As was indicated previously, the steady state temperature is somewhat higher than the environmental temperature. The thermal leakage modulus, M_T, is expressed thus:

$$M_T = \frac{dT}{dt} \Big/ (T_{actual} - T_{ss})$$

where T_{actual} and T_{ss} are the actual temperature of the calorimeter and the steady state temperature respectively. To a sufficiently good approximation, the resistance of the thermometer varies linearly with temperature so the leakage modulus can be expressed as an "ohmic leakage modulus", M_Ω,

$$M_\Omega = \frac{dR}{dt} \Big/ (R_{actual} - R_{ss})$$

where R_{actual} and R_{ss} are the actual decade setting and the decade

setting at T_{ss} respectively. M_Ω and R_{ss} are calculated from the fore-slope and after-slope which are expressed as the number of chart divisions the track crosses per unit time. Since the chart flow-rate is constant and the sensitivity is known, the slopes are expressed as ohms per millimeter. The fore-slope is extrapolated to the beginning of the reaction and the after-slope extrapolated to the end of the reaction. These two extrapolation points differ in time by the duration of the reaction; and also, usually, by a certain number of divisions which is corrected for as it was with each heat input. (See Fig. 7) In this case the difference was -4.9 div. or -2.05Ω. R_a is then 3793 - 2.05 or 3790.95Ω.

Thus for our example:

$$\text{fore-slope} = \frac{-19.6 \text{ div}}{100\text{mm} \times 2.514 \frac{\text{div}}{\Omega}}$$

$$= - 0.07796 \frac{\Omega}{\text{mm}}$$

$$\text{after-slope} = \frac{+ 33.0 \text{ div}}{100\text{mm} \times 2.388 \frac{\text{div}}{\Omega}}$$

$$= + 0.1382 \frac{\Omega}{\text{mm}}$$

$$M_\Omega^f = \frac{dR_f}{dt} \Big/ (R_f - R_{ss})$$

$$= - 0.07796 / (3334 - R_{ss}) \quad \text{mm}^{-1}$$

$$M_\Omega^a = \frac{dR_a}{dt} \Big/ (R_a - R_{ss})$$

$$= + 0.1382 / (3790.95 - R_{ss}) \quad \text{mm}^{-1}$$

$M_\Omega^f = M_\Omega^a$, so:

$$(3790.95 - R_{ss}) = - 1.773 (3334 - R_{ss})$$

$$2.773 R_{ss} = 9702.13$$

$$R_{ss} = 3498.78 \Omega$$

$$(R_f - R_{ss}) = - 164.78 \Omega$$

$$(R_a - R_{ss}) = + 292.17 \Omega$$

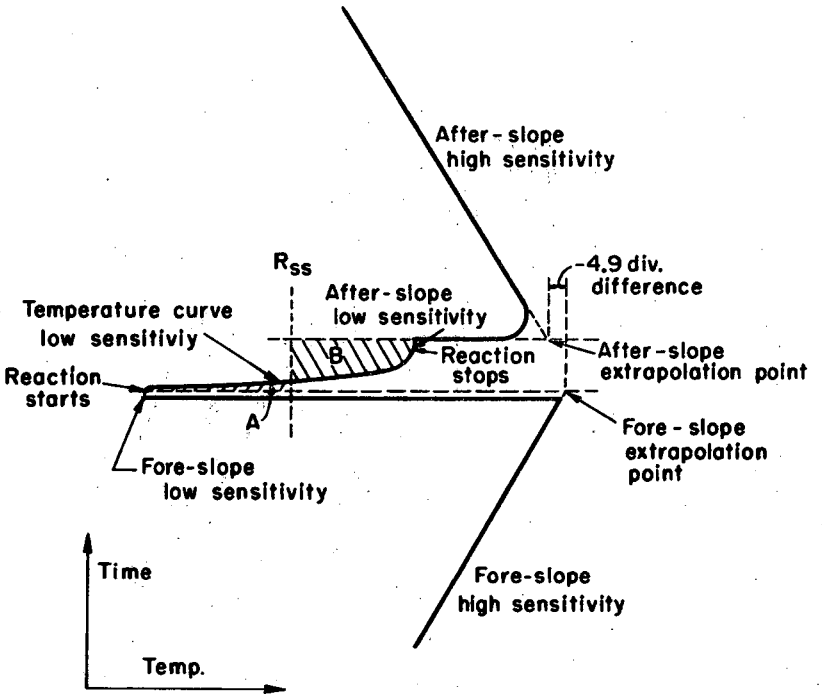

Fig. 7. Recorder track for dissolution of magnesium in 1.0μ HCl.

$$M = \frac{0.1382 \frac{\Omega}{mm}}{292.17\ \Omega}$$

$$= 4.730 \times 10^{-4}\ mm^{-1}$$

As was mentioned previously, the potential divider permits monitoring the temperature curve during the reaction. The curve in this example goes across the T_{ss} as is indicated by the change in sign of the slope, and the position of R_{ss} on the high sensitivity and the sensitivity ratio. This ratio is 11. Thus:

$$\frac{\text{Sensitivity ratio}}{\text{High sensitivity } \frac{div}{\Omega} \times \frac{mm}{div}} = \text{Low sensitivity } \frac{\Omega}{m}$$

$$\frac{11}{2.451 \frac{div}{\Omega} \quad 2.1 \frac{mm}{div}} = 2.137 \frac{\Omega}{m}$$

Here $2.451 \frac{div}{\Omega}$ is the average of the high sensitivities before and after the reaction

$$R_{ss} - R_f = 164.78\ \Omega$$

and

$$\frac{164.78 \Omega}{2.137 \frac{\Omega}{mm}} = 77.1\ mm$$

Thus R_{ss} can be drawn across the temperature curve 77.1 mm up-scale from R_f on the low sensitivity. This is shown in Fig. 7. The areas A and B represent the heat that leaked into and out of the calorimeter respectively, and are measured by superimposing thin mm graph paper on the chart and counting squares. The low sensitivity value in ohms per mm times the leakage modulus gives the number of ohms per square millimeter. This factor times the net area, (B - A), gives us the number of ohms to be added to R_a for the heat leak correction.

$$2.137 \frac{\Omega}{mm} \times 4.730 \times 10^{-4}\ mm^{-1} = 1.011 \times 10^{-3} \frac{\Omega}{mm^2}$$

$$(B - A) = +1671\ mm^2$$

$$\text{correction} = 1.011 \times 10^{-3} \frac{\Omega}{mm^2} \times 1671\ mm^2$$

$$\text{correction} = +\ 1.69\ \Omega$$

$$\text{and } R_a = 3790.95 - 1.69$$

$$= 3792.64\ \Omega$$

The fractional change is 2.76296×10^{-4}. Dividing this by the average fractional change per calorie of the several heat inputs gives the net heat of the reaction:

$$\frac{2.7630 \times 10^{-4}}{3.7553 \times 10^{-4}\ \text{cal}^{-1}} = 0.73576\ \text{cal}$$

As was previously mentioned, this net heat value must be corrected for the heat of breakage of the sample bulb, and the heat of vaporization of the solution into the dry hydrogen evolved and the air in the bulb. The heat of vaporization of water is used to approximate the heat effect in the one molar hydrochloric acid used and is 10,480 calories per mole. Thus one calculates for the heat of vaporization of water into the dry hydrogen 0.002157 cal., and into the air in the bulb at 44% relative humidity 0.000201 cal. The heat of breakage is 0.000560 cal. Thus the heat of solution of 161.29 μg of pure Mg metal in 1.00M HCl is 0.73756 cal. or $\Delta H_{298} = -111.2$ Kcal/mole. Table 1 gives the corrected results for four runs.

TABLE I

Heat of the Reaction $Mg + 2H^+ \longrightarrow Mg^{++} + H_2\uparrow$

	Sample Weight (μg)	Heat Evolved (calories)	ΔH_{298} (Kcal/mole)
1.	51.97	0.2377	-111.2
2.	65.85	0.3023	-111.6
3.	84.17	0.3846	-111.1
4.	161.29	0.7375	-111.2
		Average	-111.3 ± 0.2

Shomate and Huffman's value is -111.322 ± 0.041. The results indicate that there are no significant systematic errors and that the precision of the operation is about 0.2%.

III. MATERIALS

A. Europium Metal

Europium metal can be obtained commercially in quite high purity: 99.9% with respect to all contaminants, is claimed. One sample of metal was quite pure spectrographically, but contained small, random inclusions of a reddish powder. The nature of this powder is unknown, but it rendered the metal unsuitable for use as calorimeter samples. A second metal sample from the same firm was double distilled, but still showed the red inclusions, this time in the form of thin red streaks instead of pockets. An attempt was made to "slag" this "two-phase" metal by packing a small Ta crucible with chunks and melting under high vacuum. There was very little separation of the inclusions from the metal, and only a very small portion at the top of the resulting ingot proved satisfactory for calorimeter samples.

A small rod of europium metal was kindly furnished us by Professor Frank Spedding, and this proved to be quite satisfactory, One end of this rod was free of any visual contaminant. The chemical purity data for this sample are given in Table II. All Eu metal calorimeter samples were taken from this rod.

The samples were cut and mechanically cleaned in a dry nitrogen "inert atmosphere" glove box. The nitrogen was obtained by boiling liquid nitrogen to flush the box for 16 to 18 hours. The box atmosphere was then recycled through a liquid nitrogen trap to remove water, and a copper wool furnace at 600°C to remove oxygen. Under optimum conditions, freshly cut europium could be held free of tarnish for about two hours. Longer exposure to the box atmosphere would generate a faint golden tarnish. No samples were free of tarnish because of the extreme reactivity of europium and the imperfect box atmospheres, but

TABLE II

Analysis of Europium Metal

(results expressed as %)

Al < 0.01	Gd < 0.05	Sc < 0.01
Ba < 0.01	Ho < 0.05	Si < 0.01
Ca < 0.01	La < 0.01	Ta < 0.1
Nb < 0.01	Lu < 0.05	Tb < 0.5
Ce < 0.05	Mg < 0.01	Tm < 0.05
Dy < 0.05	Na < 1	Yb < 0.01
Er < 0.05	Nd < 0.1	Y < 0.01
Fe < 0.01	Pr < 0.5	Zr < 0.01

the variations in tarnish realized did not affect the precision of the results outside of experimental error. It is assumed that an absolutely tarnish-free sample would yield results that differ from those obtained by less than the experimental error.

B. Europium Monoxide

Europium monoxide was prepared by direct combination of the metal and the sesquioxide, both 99.9% pure, in vacuum at high temperature in a sealed tantalum crucible in one method, and in a closed but unsealed tantalum crucible in the other. (See Fig. 8.)

The unsealed system contained a portion of oxide, and a 5% stoichiometric excess of metal according to the reaction:

$$1.05\ Eu + Eu_2O_3 \rightarrow 3\ EuO + 0.05\ Eu \qquad (1)$$

The oxide was pretreated by heating in an oxygen atmosphere overnight[3] at 400°C to remove carbonate and absorbed gases. The oxide was then stored under dry argon. The metal was cut and cleaned in the inert atmosphere box, sealed in a small tared glass bulb, and weighed on an Ainsworth Type V.M. Assay balance to 0.01 mg. The corresponding amount of Eu_2O_3 was calculated, weighed, and combined with the metal in the crucible in the dry box. The lid was set in place and the crucible, suspended in an induction shield, was loaded in the vacuum line. The system was carefully outgassed by gentle heating with a R.F. induction heater until the temperature could be raised with no increase in pressure.

The crucible was then heated in high vacuum at from 1400°C to 1550°C for about four hours at a pressure in the low 10^{-6} mm Hg range. The crucible was opened in the dry box and the reddish-brown crystalline powder removed. The analytical data on four preparations by this method are given in Table III, numbers 1, 2, 3, and 4.

Preparations 5, 6, and 7 were made in sealed systems. A heavy-walled tantalum crucible with a properly machined lid[4] for subsequent heliarc welding was used. The europium metal was cut, cleaned, and weighed as before; and the exactly stoichiometric amount of Eu_2O_3 calculated, weighed out, and combined with the metal in the crucible.

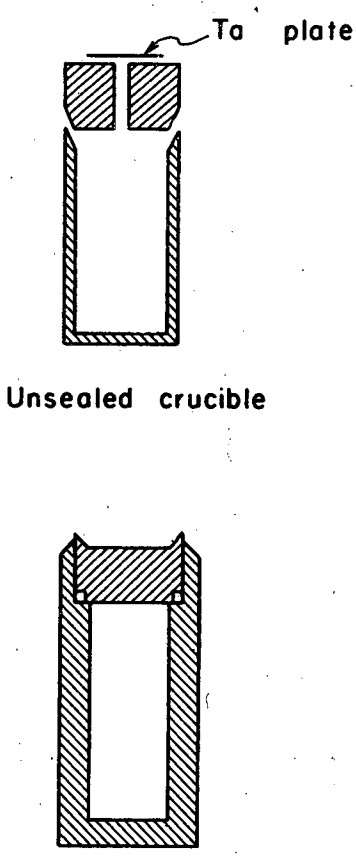

Fig. 8. Tantalum crucibles.

TABLE III

EuO Preparations Analyses

No.	Lattice Parameter	Stoichiometry
1.	a_o = 5.1429 Å	O/Eu = 1.022, 1.020, 1.022, 1.019 = 1.021 ± 0.001
2.	a_o = 5.1428 Å	O/Eu = 1.013, 1.009, 1.007, 1.010 = 1.010 ± 0.002
3.	a_o = 5.1429 Å	O/Eu = 1.022, 1.035; 1.176*, 1.299*
4.	a_o = 5.1430 Å	O/Eu = 1.04, 1.02, 1.02, 1.02 = 1.02 ± 0.01
5.	a_o = 5.1435 Å	O/Eu = 1.030, 1.026, 1.027 = 1.028 ± 0.002
6.	a_o = 5.1477 Å	O/Eu = 1.017, 1.038; 1.334*, 1.332*
7.	a_o = 5.1432 Å	O/Eu = 1.04, 1.05, 1.07, 1.04 = 1.05 ± 0.02
8.	a_o = 5.144 Å	
9.	a_o = 5.1419 Å	*listed lattice parameter does not apply to these numbers
10.	a_o = 5.1421 Å	
11.	a_o = 5.1431 Å	
12.	a_o = 5.1430 Å	

The lid was then welded on and the system leak checked at room temperature. It was heated as before but cooled slowly: reduced to about 800°C over a three-hour interval. All samples proved to be 99.9% pure spectrographically.

Each preparation appeared to be inhomogeneous to a certain degree. They all exhibited an occasional small pocket of a bright yellow powder. The periphery of the pocket was a dark wine color which faded into the reddish-brown color of the major phase. The nature of these inclusions is unknown, but they are probably europium-oxygen combinations of varying composition. The amount of the inclusions was estimated at less than 0.1% of the major phase. When the agglomerated pieces were broken up to yield chunks of a size suitable for the calorimeter runs, the inclusions could be removed. Preparations numbered 3. and 6. showed substantial portions, 15 to 20%, of a second phase which was significantly darker in color than the other phase, and was not as well agglomerated nor as lustrous. Powder patterns of samples from each of these portions agree with each other, but show no EuO lines. Achard[5] mentions a phase with an O/Eu ratio of 1.3 calculated from x-ray evidence. Bärnighausen and Brauer[6] report a new europium oxide with the composition Eu_3O_4 made from an equal-molar mixture of EuO and Eu_2O_3 heated to 900°C for 2 hours under a pure inert gas. The formula was determined by comparing the intensities and positions of the powder pattern lines with those of Eu_2SrO_4. Both substances are orthorhombic with the following lattice parameters:

	Eu_3O_4	Eu_2SrO_4
a	10.094 Å	10.133 Å
b	12.068	12.081
c	3.500	3.4979

The squares of the sines of the angles of diffraction calculated from Brauer's data are not in complete agreement with those observed here; therefore, it is not claimed that the second phase observed here is pure Eu_3O_4. No further characterization of this phase has been done by this author.

The oxygen-to-europium ratios shown in Table III were obtained by igniting a known weight of sample to constant weight of Eu_2O_3. From ten to twenty milligrams of "EuO" were weighed in small quartz weighing bulbs to a hundredth of a milligram on the Ainsworth Type V.M. Assay balance. The bulbs were loaded in a dry box and were fitted with small glass stoppers to minimize contact of the sample with the air during weighing. They were then ignited at 700°C in air; the weight increases were measured on the previously mentioned torsion balance and were from one-half to more than one milligram. The ignition product powder pattern agreed with the monoclinic phase of Eu_2O_3. In Preparations 3. and 6. it was intended to determine the stoichiometry of both the usual reddish-brown phase and the other or dark brown phase. In each case the first two values are for the reddish-brown phase.

Concerning this phase it is noted that the lattice parameters for the several preparations are essentially constant with the exception of number 6. These can be compared with the value from a sample from Los Alamos Scientific Laboratory: 5.1443 Å. The literature values include 5.1439 Å,[7] 5.141 Å,[8] and 5.14 Å[5].

Monoxides can crystallize with one or more of three different crystal structures: sodium chloride, zinc blende, or wurtzite with some variations and defect structures. In the NaCl form, each atom is octahedrally coordinated; while in the zinc blende and wurtzite structures the coordination is tetrahedral. This difference can be seen in the

powder pattern of the sample in the relative intensities of the following pairs of reflections: 111,200; 311,220; 331,420. The x-ray data for Preparation 2 is presented in Table IV. The observed relative intensities of the three pairs of reflections agree with the calculated values indicating a NaCl type face-centered cubic structure for EuO. This is also the case for the alkaline-earth oxides and the monoxides of many of the transition metals. The literature contains data on other lanthanide monoxides: LaO—5.249 Å,[9] CeO—5.11 Å,[10] NdO—5.068 Å,[11] SmO—4.9883 Å,[7] YbO—4.86 Å,[5] all of which are fcc NaCl type. Within the accuracy of the results in Table III, nothing definite can be said concerning the correlation between lattice parameter and the O/Eu.

All the europium monoxide analyses known to this observer have shown a non-stoichiometric composition. This includes the one sample from the Los Alamos Scientific Laboratory where the O/Eu was 1.009. The latter preparation consisted of the stoichiometric combination of Eu and Eu_2O_3 in a Ta capsule welded shut under high vacuum and then heated at 1650°C for 8 hours. The lattice parameter measured 5.1443 Å.

As the data are presented, an excess of oxygen is indicated; but this can also be represented as a deficiency of europium: an oxygen lattice with some vacancies in the octahedral positions. "Iron monoxide, FeO", presents just such a case.[12] Oxides with O/Fe from 1.06 to 1.19 show a decrease in density and unit cell volume with increasing oxygen content indicating iron deficiency. The composition can be expressed $Fe_{0.94}O$ to $Fe_{0.84}O$.

"Manganese monoxide" has shown a composition range with the O/Mn from 1.0056 to 1.044.[13] It was referred to as having cation vacancies, thus the formula range is $Mn_{0.994}O$ to $Mn_{0.957}O$. "Vanadium monoxide"

TABLE IV

Powder Pattern Data for EuO Preparation 2.

Reflection		θ	hkl	$\sin^2$ θ obs.	$\sin^2$ θ calc.	Intensity obs.	Intensity calc.
1		15.08	111	0.06769	0.0674	S	100.00
2		17.45	200	0.08992	0.0899	S-	79.63
3		25.13	220	0.18034	0.1797	M	55.44
4		29.83	311	0.24744	0.2471	M-	45.85
5		31.30	222	0.26990	0.2696	W	18.68
6		36.88	400	0.36017	0.3595	T	8.60
7	α_1	40.78	331	0.42662	0.4262	M-	19.67
8	α_2	40.93		0.42921	0.4283		
9	α_1	42.05	420	0.44861	0.4486	M	24.67
10	α_2	42.18		0.45086	0.4508		
11	α_1	47.23	422	0.53889	0.5383	M-	20.08
12	α_2	47.38		0.54149	0.5410		
13	α_1	51.10	511 333	0.60566	0.6056	M	19.00
14	α_2	51.28		0.60873	0.6086		
15	α_1	57.93	440	0.71809	0.7178	W	9.57
16	α_2	58.13		0.72123	0.7213		
17	α_1	62.38	531	0.78507	0.7851	M+	32.63
18	α_2	62.68		0.78936	0.7890		
19	α_1	63.98	442	0.80755	0.8075	M	22.04
20	α_2	64.30		0.81195	0.8115		
21	α_1	71.33	620	0.89753	0.8972	M	30.06
22	α_2	71.73		0.90172	0.9017		
23	α_1	79.18	533	0.96476	0.9645	M	41.58
24	α_2	79.90		0.96924	0.9693		

has a homogeneous NaCl type phase over the composition range: O/V = 0.80 to 1.20, showing random vacancies for both cations and anions.

The failures of the attempts to prepare the exactly stoichiometric compound may indicate its instability at the preparation temperatures. There is also the possibility that there is an appreciable vapor pressure of europium over the oxide phase which does not re-equilibrate with the substrate upon cooling. Achard[5] reports that EuO can be distilled at 1700°C in vacuum without decomposition, yielding a distillate of unchanged structure and lattice parameter. There is the possibility that his vaporized species was really europium metal which was oxidized to EuO by residual oxygen in the system, but in a well degassed system this possibility is unlikely. He did not say at what pressure the distillation took place. Stoichiometric analysis of the substrate would indicate the vaporization process.

The material used for the calorimetric analyses was Preparation 1: $EuO_{1.021}$. For the purposes of calculation, it was considered to be an ideal solid solution of Eu_2O_3 in EuO, but this is almost certainly not the case. It is thus represented as $EuO \cdot 0.021 Eu_2O_3$.

Calorimeter samples of Eu and EuO were of about 500μg mass and were prepared as was described previously. This sample size was chosen because of certain limitations imposed by the microcalorimeter.

C. Solutions

The solutions of HCl used were prepared from analytical grade reagents. The solutions used for the Eu metal calorimeter runs were 0.1 N HCl saturated with O_2 gas. Those for EuO were 1.0N HCl saturated with O_2 gas. The function of the O_2 gas will be discussed later.

IV. CALORIMETRIC MEASUREMENTS

A. Europium Metal

The experimentally observed heats of solution of europium metal in oxygen-saturated hydrochloric acid are given in Table V.

For accurate calculations, a well-defined calorimeter reaction is of primary importance. In the case of europium there can be some uncertainty depending on the composition of the solution at the start of the reaction. When the solution is saturated with oxygen gas the reactions are considered to be:[14]

$$Eu + 2H^{+} \rightarrow Eu^{+2} + H_2 \qquad (2)$$

$$Eu^{+2} + H^{+} + \tfrac{1}{4}O_2 \rightarrow Eu^{+3} + \tfrac{1}{2}H_2O \qquad (3)$$

and for the total reaction:

$$Eu + 3H^{+} + \tfrac{1}{4}O_2 \rightarrow Eu^{+3} + \tfrac{1}{2}H_2O + H_2 \qquad (4)$$

In acid solutions there is one other competing reaction for the oxidation of Eu^{+2}:

$$Eu^{+2} + H^{+} \rightarrow Eu^{+3} + \tfrac{1}{2}H_2 \qquad (5)$$

But in considering the relative reaction rates, reaction (3) is much faster than (5). Samples of europium metal were dissolved in argon-flushed media and the absorption spectrum taken with a Cary Model 14 Recording Spectrophotometer. These solutions showed strong absorption in the ultraviolet: with the europium concentration approximately thousandth molar, the optical density was greater than 2.0 at wave lengths less than 3000 Å. However, in an oxygen-flushed medium there was no such absorption. Depending on the efficiency of the argon flush, the absorption persisted to a measurable extent for more than two hours, whereas the heat evolution of the reaction in an oxygen-saturated medium in the calorimeter was complete in 1 to $1\frac{1}{2}$ minutes.

The hydrogen gas evolved from the solution of samples of La and Eu

TABLE V

Heat of Solution of Europium Metal in O_2 sat'd. 0.1N HCl

	Sample Weight (μg)	Eu^{+3} Molarity	Heat Evolved (cal)	$\Delta H_{298.2}$ (Kcal/mole)
1.	403.4	3.318×10^{-4}	0.4376	-164.85 ± 0.6
2.	400.5	3.294×10^{-4}	0.4347	-164.94 ± 0.6
3.	462.4	3.802×10^{-4}	0.4987	-163.91 ± 1.0
4.	546.6	4.496×10^{-4}	0.5925	-164.77 ± 1.0
			Average	-164.62 ± 1.0

metals in oxygen-saturated 0.1N HCl was measured and found to yield hydrogen-to-metal mole ratios of 1.53 and 1.02 respectively. Thus it is claimed that in oxygen-saturated acid, reaction (5) proceeds to a negligible extent; so the calculations are based on reaction (4).

It was also attempted to run europium metal in an oxygen-free medium thus eliminating reaction (3); and since reaction (2) is much faster than reaction (4), the heat effect due to reaction (2) can be measured which, except for small corredtions, is just the heat of formation of $Eu^{+2}_{(aq)}$.

Maintaining an oxygen-free solution proved to be rather difficult. Simply flushing the acid with argon and loading in an inert atmosphere proved to be inadequate because the solution in the calorimeter is open to the atmosphere along the stirring shaft. Since there is a small clearance between the shaft and the guide in the hanger, a mercury droplet was used to fill a small space around the shaft above the guide. The mercury would not drop through the small clearance. In addition an "oxygen scavenge" was put in with the flushed acid when the run was loaded. The "scavenge" was a small piece - about one milligram - of europium metal which would provide europous ions to react with the residual oxygen. But since the mercury does not wet the shaft and hanger, there was still a small leak which consumed all the scavenge during the long pump-down time. However, if an appreciably larger scavenge - about six milligrams - was used, the solution could be maintained oxygen free for a sufficiently long period of time.

However, the heats of solution of europium metal in such solutions varied considerably. Visual observation of europium metal dissolved in oxygen-free hydrochloric acid revealed a residual white material that could be centrifuged. The solution would also exhibit a Tyndall beam. Thus the calorimeter reaction is not defined. The nature of

this white material is unknown, but it is possibly a polymeric hydrated europous oxide or europous hydroxide. In the immediate vicinity of the dissolving metal, the pH is probably quite high, as the hydrogen ions are consumed; this could lead to the hydrolysis of the Eu^{+2} formed and subsequent polymerization of the hydrolysis product, which is only slowly attacked by hydrogen ion. There is also the possibility of the oxidation of Eu^{+2} to Eu^{+3} by H_2O with hydrolysis of the Eu^{+3} as Eu^{+3} hydrolyses more readily than Eu^{+2}. The polymer formed then could be one containing Eu^{+3}.

The situation is thermodynamically quite different when oxygen is plentiful in the solution: $Eu^{+2}_{(aq)}$ is no longer so stable and the dissolution proceeds much more rapidly to completion.

The calorimeter reaction may be better defined if the europium sample is already as Eu II. For this case we used "europium monoxide" which is described in the next section.

B. "Europium Monoxide"

The experimental values for the heat of solutions of "europium monoxide" in oxygen-saturated hydrochloric acid are tabulated in Table VI.

It was found that the "EuO" did not dissolve as readily in 0.1N HCl as the europium metal, but instead required 2 to 3 minutes; a suitably fast dissolution was obtained in 1.0N HCl, however. As in the case of the metal, these solutions were saturated with oxygen gas to define the calorimeter reaction:

$$EuO{\cdot}0.021Eu_2O_3 + 2.126H^+ \rightarrow Eu^{+2} + 0.042Eu^{+3} + 1.063H_2O \quad (6)$$

$$Eu^{+2} + H^+ + 0.25O_2 \rightarrow Eu^{+3} + 0.5H_2O \quad (7)$$

and for the total reaction:

$$EuO{\cdot}0.021Eu_2O_3 + 3.126H^+ + 0.25O_2 \rightarrow 1.042Eu^{+3} + 1.563H_2O \quad (8)$$

The uncertainty in the average value for the heat of solution of $EuO_{1.021}$ is rather large and indicates a degree of inhomogeneity in the material. This is not noticed in the stoichiometric measurements because there the sample size was about forty times larger, whereas the calorimeter samples were chunks of the proper size chosen at random from the broken-up agglomerate.

As was mentioned previously, "EuO" was used in an attempt to determine the heat of formation of $Eu^{+2}_{(aq)}$. The oxygen-free solutions were prepared by running a solution 0.005N in Eu^{+3} and 1N in HCl through a Jones Reductor and loading in an inert atmosphere. The solutions thus prepared provided very conveniently an oxygen-free solution with sufficient Eu^{+2} scavenge. The expected calorimeter reaction is then reaction (6) from which the heat of formation of $Eu^{+2}_{(aq)}$ can be calculated.

However, reproducibility in the heats of solution was very poor,

TABLE VI

Heat of Solution of $EuO_{1.021}$ in O_2 sat'd. 1.0N HCl

	Sample Weight (μg)	Eu^{+3} Molarity	Heat Evolved (cal)	$\Delta H_{298.2}$ (Kcal/mole)
1.	439.3	2.61×10^{-4}	0.2936	-87.7 ± 0.8
2.	414.2	2.46×10^{-4}	0.2311	-89.8 ± 0.7
3.	359.5	2.13×10^{-4}	0.1957	-87.5 ± 0.7
4.	305.0	1.82×10^{-4}	0.1636	-86.3 ± 0.6
			Average	-87.8 ± 1.7

and the values for the heat of formation of Eu^{+2} appeared to be about 15 Kcal too negative, as compared with the calculated value. Here, as in the case with europium metal mentioned previously, the calorimeter reaction does not appear to be well-defined. The dissolution rate in this case is much slower — 7 to 10 minutes — so the increase in pH around the sample may not be as rapid, but since the starting material is already the oxide, the conditions for formation of a hydrated oxide polymer may still be favorable.

It is recommended that $EuCl_2$ be used for the determination of the heat of formation $Eu^{+2}_{(aq)}$ as it is readily soluble without change in pH. The heat of solution in oxygen-saturated HCl would yield the heat of formation of $EuCl_{2(c)}$; this value and the heat of solution in oxygen-free HCl would yield the heat of formation of $Eu^{+2}_{(aq)}$.

V. RESULTS AND DISCUSSION

The calorimetric measurements of the heat of solution of europium metal in oxygen-saturated 0.1N HCl permit the calculation of the standard heat of formation of $Eu^{+3}_{(aq)}$. If we subtract from the average heat of solution given in Table V the heat of formation of one-half mole of water,[15] neglect the slight change in the composition of the HCl solution due to consumption of H^+ in the dissolution of the metal, and approximate the state of infinite dilution by 0.1N HCl, we obtain

$$\Delta H^{o}_{fEu^{+3}_{(aq)}} = -130.4 \pm 1.0 \text{ Kcal/mole.}$$

A plot of the experimental heats of formation of aqueous tripositive lanthanide ions is given in Fig. 9.[16,17,18]

It is noted that the heat of formation of $Eu^{+3}_{(aq)}$ is some 33 to 34 Kcal more positive than the values for $Sm^{+3}_{(aq)}$ or $Gd^{+3}_{(aq)}$, but it should also be noted that europium metal is very unlike either Sm or Gd. Some of the pertinent physical properties of the lanthanide metals are included in Table VII.[19] For each of the properties listed, Eu and Yb are the anomolies.

Fig. 9 indicates that for most of the rare earths there is roughly a linear decrease of only about 0.8Kcal/mole per atomic number in the heats of formation of the aqueous tripositive ions. Hence, for these elements, the terms in the Born-Haber cycle:

$$M_{(c)} \rightarrow M_{(g)} \rightarrow M^{+3}_{(g)} + 3e^- \xrightarrow{3H^+_{(aq)}} M^{+3}_{(aq)} + 3/2H_{2(g)}$$

must sum to the same value within a few kilocalories.

Values for the first ionization potential are tabulated[19] for most of the lanthanides, but only for lanthanum are the first three known.[19] The sum of the first three ionization potentials for the

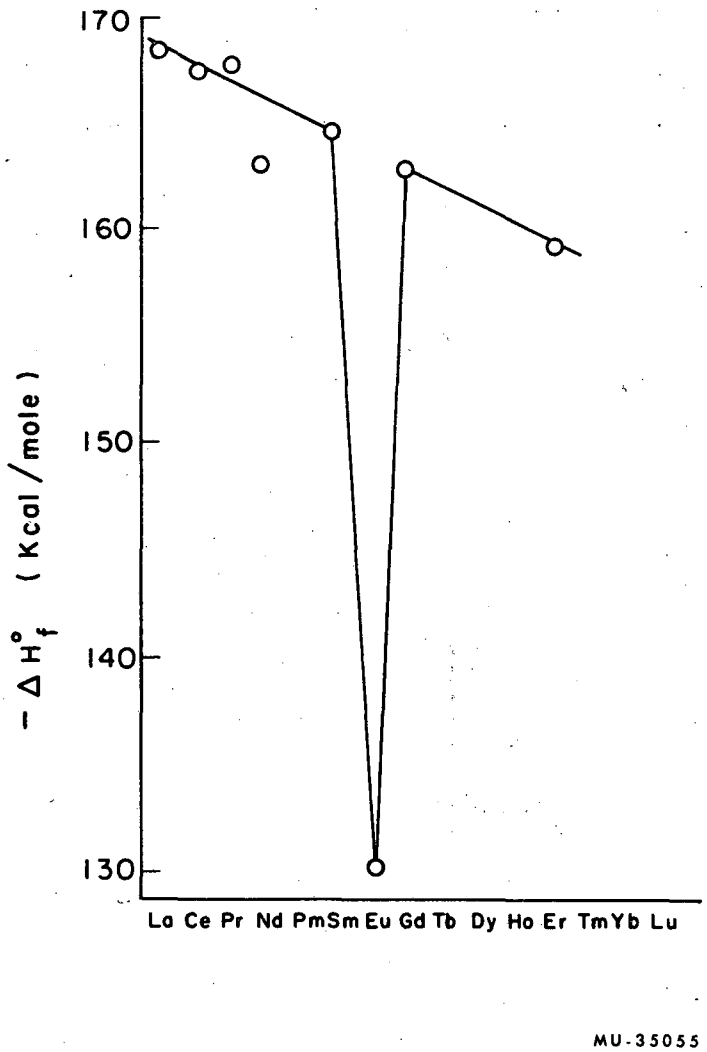

Fig. 9. Heats of formation of aqueous tripositive lanthanide ions.

TABLE VII

Some Physical Properties of Lanthanide Metals

	Met. Valence	M.P. °C	$\Delta H^{o}_{sub.}$ Kcal/mole	g/cc	Met. Rad. Å	cc/mole
La	3	920	99.5	6.18	1.88	22
Ce	3.1	797	97.6	6.79	1.83	21
Pr	3	935	84.7	6.48	1.84	21
Nd	3	1024	75.6	6.96	1.83	21
Pm	3	-	-	-	-	-
Sm	2.9	1072	50.6	7.50	1.81	20
Eu	2.1	826	42.2	5.30	2.04	29
Gd	3	1312	81.3	7.96	1.81	20
Tb	3	1356	(72)	8.25	1.78	19
Dy	3	1407	69.8	8.45	1.77	19
Ho	3	1461	75.0	8.76	1.77	19
Er	3	1497	75.4	9.04	1.76	18
Tm	3	1545	58.4	9.27	1.75	18
Yb	2.0	824	41.5	7.02	1.96	25
Lu	3	1652	94.0	9.81	1.73	18

rest of the lanthanides can be calculated from the Born-Haber cycle with values for the standard heats of formation of the aqueous tripositive ions, the heats of sublimation, and the heats of hydration of the gaseous tripositive ions.

The heats of hydration can be estimated from the Born equation

$$E = \frac{q^2}{2r}\left(1 - \frac{1}{D}\right)$$

where q is the charge on the ion in esu, r is the radius of the hydrated ion in centimeters, and D is the dielectric constant of water. In the neighborhood of the charged particle, the dielectric constant is probably much different from the bulk value of 78, but unless the value is drastically different from 78, the $(1 - \frac{1}{D})$ term effects the energy by only about a percent.

A measure of the radius of the hydrated ion is the ionic conductance at infinite dilution. The trend of the hydrated radii is the inverse of the trend of the ionic conductances, if Stokes Law for the flow of a particle through a viscous medium is assumed to approximate the case. If the radius of one ion can be determined, the others can be inferred from conductance data. Only in the case of lanthanum are the necessary data available for the calculation of the radius of the hydrated tripositive ion.

The heat of hydration of $La^{+3}_{(g)}$ can be calculated from the sum of the first three ionization potentials, the heat of sublimation, and the standard heat of formation of $La^{+3}_{(aq)}$ using the Born-Haber cycle:

$$\Delta H_{Hyd.} = \Sigma \text{ I.P.} + \Delta H_{sub.} - \Delta H^{\circ}_{f La^{+3}}$$

$$= 835 + 100 + 169$$

$$= 1104 \text{ Kcal.}$$

With this value and the Born equation, and using 78 for the dielectric constant of water, the radius of the hydrated tripositive lanthanum ion can be calculated:

$$1104 = \frac{(3 \times 4.80 \times 10^{-10})^2}{2r}\left(1 - \frac{1}{78}\right)\frac{6.023 \times 10^{23}}{4.184 \times 10^{7}}$$

$$r^{La^{+3}}_{Hyd.} = 1.36\text{Å}$$

Conductance data on several rare earth salts are available[20] and the ionic conductances of the tripositive rare earth aqueous ions have been tabulated.[21] These show a decreasing trend indicating an increasing hydrated radius, as would be expected. The hydrated radius of any lanthanide tripositive ion can then be expressed as the ratio of the ionic conductance of $La^{+3}_{(aq)}$ to that of the other ion times the radius of $La^{+3}_{(aq)}$.

The heats of hydration of the gaseous tripositive ions can now be estimated, and for those lanthanides for which the heat of formation of the aqueous tripositive ion is known, the sum of the first three ionization potentials can be calculated. All these data are tabulated in Table VIII, and a plot of the heats of hydration and sums of the first three ionization potentials is given as Fig. 10.

The calculation of the hydrated radii is admittedly empirical. One would expect the radius of the aqueous ionic species to be nearly approximated by the sum of the crystallographic ionic radius plus the length of the associated water dipoles in the first hydration sphere. In the case of lanthanum this sum would be around four angstroms, but then one encounters large inconsistancies in the calculated values for the hydration energy.

For the purpose of the present consideration, suffice it to say that the resulting ionization potential sum does show the expected

TABLE VIII

	La	Ce	Pr	Nd	Sm	Eu	Gd	Tb	Dy	Ho	Er	Tm	Yb	Lu
Ionic cond. at∞ dil.	69.3	69.9	69.2	69.5	68.2	67.9	67.0		65.7	66.0	65.8	65.5	65.4	
$\frac{\text{I.C. } La^{+3}_{(aq)}}{\text{I.C. } M^{+3}_{(aq)}}$	1.000	0.991	1.001	0.997	1.016	1.021	1.034		1.055	1.050	1.053	1.058	1.060	
$r^{M^{+3}}_{Hyd.}$	1.36	1.35	1.36	1.36	1.38	1.39	1.41		1.43	1.43	1.43	1.44	1.44	
$-\Delta H_{Hyd.}$ Kcal.	1104	1111	1104	1104	1087	1079	1064		1049	1049	1049	1042	1042	
$\Delta H_{sub.}$ Kcal.	100	98	85	76	51	42	81	(72)	70	75	75	58	42	94
$-\Delta H_{fM^{+3}_{(aq)}}$ Kcal.	169	167	168	163	164	130	163				159			
I. P. Kcal.	835	846	851	865	872	907	820				815			
I. P. e.v.	36.2	36.7	36.9	37.5	37.8	39.3	35.6				35.3			

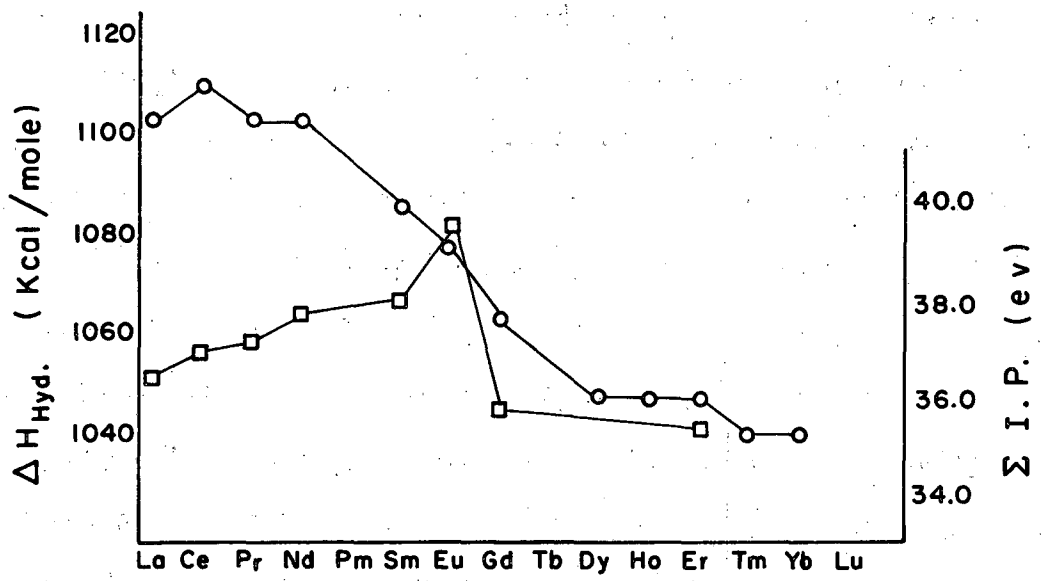

Fig. 10. Heats of hydration of $M^{+3}_{(g)}$ —o— o—
Σ First three I.P. —□—□—

trend through Sm, and the peak at Eu and drop to Gd are significant, even through the absolute value may be in error.

The formation of $Eu^{+3}_{(g)}$ involves the breaking of the relatively stable half-filled 4f shell of electrons. If the trend through Sm is continued through Eu, the value for Eu is about 38 e.v. which indicates that the additional stabilization energy of the electron that completes the half-filled 4f shell is about 1.3 e.v. or 30 Kcal. Jørgensen[22] has given an expression from which this energy can be calculated. He says that the differences between the values of the expression $DS(S + 1)$ for q and $q + 1$ increase linearly with q except where $q = 2\ell + 1$, where the difference jumps to $D(2\ell + 2)$. Here D is his spin-pairing energy parameter, q is the number of 4f electrons and S and ℓ have the usual significance. The sequence of interest is tabulated in Table IX. Instead of the difference being 3.75D for q increasing from 6 to 7, as the plot would show, the difference jumps to $D(2\ell + 2)$ or 8D. So the "hump in the ionization energies" is the expected or plot value subtracted from the peak. Thus:

$$8D - 3.75D = 4.25D$$

Jørgensen's value for D in this case is 18.5 Kcals, so the theoretical value for the additional stabilazation energy for the electron that completes the half-filled 4f shell is about 80 Kcals. This is in reasonable agreement with our experimental value.

The calculated values for the sum of the first three ionization potentials for Gd and Er appear to be too low: one would expect them to be more positive than the value for Sm. What is indicated is that the configuration of Gd^{+3}, (Xe) $4f^7$, is more stable than the config-

TABLE IX

q	S	DS(S + 1)	Diff
1	1/2	0.75D	
			1.25D
2	1	2.00D	
			1.75D
3	3/2	3.75D	
			2.25D
4	2	6.00D	
			2.75D
5	5/2	8.75D	
			3.25D
6	3	12.00D	
			(3.75D) D(2ℓ + 2) or 8D
7	7/2	15.75D	
			3.25D
8	3	12.00D	

uration of La^{+3}, (Xe); and that the increase in nuclear charge of Gd and Er over La does not increase the sum of the first three ionization potentials which is almost certainly not the case.

A similar situation is seen in the 3d transition series, where, in considering the sum of the first two ionization potentials, La, Eu, and Gd are analogous to Ca, Cr, and Mn respectively. The data[23] and resulting plot are shown in Table X and Fig. 11. There is the peak at Cr, but the value for Mn is more positive than that for Ca.

Precisely why the results for Gd and Er are not as expected is not known, except that the calculations and assumptions based on La may tend to break down for the later members of the series.

The original values for the standard heat of formation of $Sm^{+3}_{(aq)}$, $Eu^{+3}_{(aq)}$, and $Yb^{+3}_{(aq)}$ were interpolated from the results obtained by H. Bommer and E. Hohmann[24] on the heats of solution of most of the rare earth metals in dilute HCl. Their metal samples were prepared by reduction of the anhydrous trichloride with potassium metal and subsequent removal of the excess potassium by distillation. The heats of solution of the mixture of metal and KCl were corrected for the heat of solution of three moles of KCl. However, Sm, Eu, and Yb were not run because of the reduction to the dichloride instead of the metal. More recent data indicate that Bommer and Hohmann's values are about 8 to 10 Kcal too negative due to the incomplete removal of potassium from the reduction product.

The value for Eu was then set at -164 Kcal/mole; and from solution measurements, the standard heat of formation of $EuCl_{3(c)}$ was considered to be about -244 Kcal/mole. This latter value is now recalculated at -210.2Kcal/mole.

TABLE X

Atomic Configurations, Ionic Configurations and Sums of First Two Ionization Potentials for First Transition Series

Atom	Atom Config.	Ion	Ion Config.	Sum First Two I.P.
Ca	$(Ar)4s^2$	Ca^{+2}	(Ar)	18.0
Sc	$(Ar)3d^1 4s^2$	Sc^{+2}	$(Ar)3d^1$	19.5
Ti	$(Ar)3d^2 4s^2$	Ti^{+2}	$(Ar)3d^2$	20.4
V	$(Ar)3d^3 4s^2$	V^{+2}	$(Ar)3d^3$	20.8
Cr	$(Ar)3d^5 4s^1$	Cr^{+2}	$(Ar)3d^4$	23.4
Mn	$(Ar)3d^5 4s^2$	Mn^{+2}	$(Ar)3d^5$	23.0
Fe	$(Ar)3d^6 4s^2$	Fe^{+2}	$(Ar)3d^6$	23.9

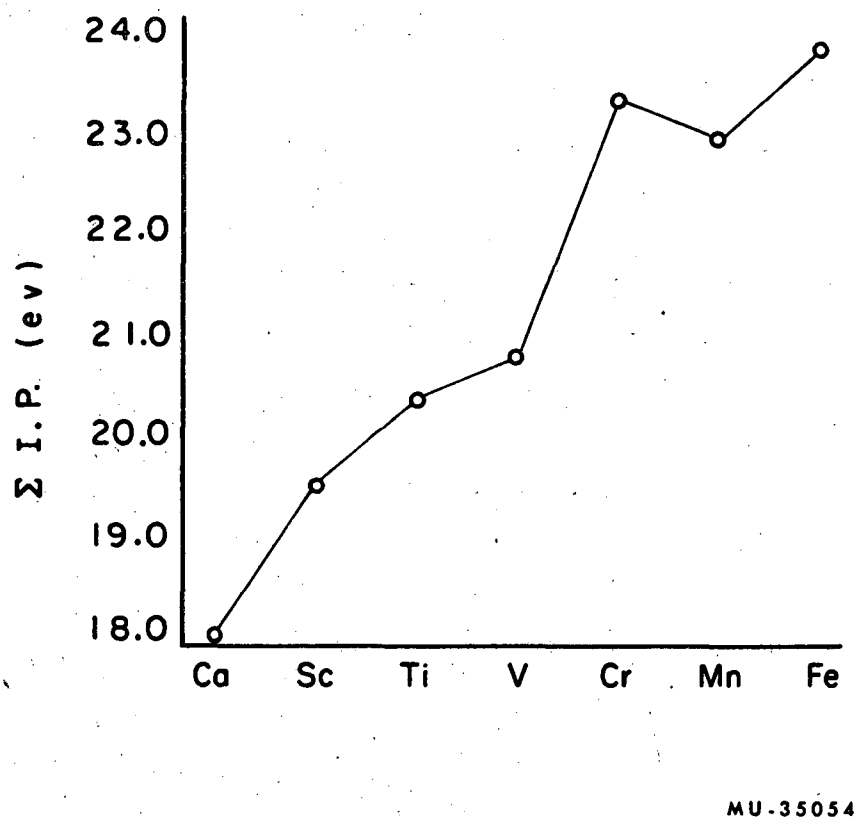

Fig. 11. Plot of sum of first two ionization potentials for part of first transition series.

The standard heat of formation of $Eu^{+2}_{(aq)}$ can be calculated from our value for the heat of formation of $Eu^{+3}_{(aq)}$, the $Eu^{+2} - Eu^{+3}$ aqueous potential, and entropy estimates for Eu^{+2} and Eu^{+3}. The value for the $Eu^{+2} - Eu^{+3}$ aqueous potential appears to be fairly well established. McCoy [25] reports 0.43 volt from an europium formate-formic acid medium. Noddack and Brukl[26] used 0.01M solutions of the rare earth sulfates in polarographic measurements and report 0.429 volt. Laitinen and Taebel[27] report 0.425 volt from polarographic studies on chloride solutions in 0.1M NH_4Cl. L.P. Shul'gin and Yu. A. Koz'min[28] give 0.428 volt in a 1N HCl solution. Entropy estimates can be made by Brewer's method[29] in which the available entropies are plotted vs. the ionic radii for divalent and trivalent ions respectively. Lewis and Randall, as revised by Pitzer and Brewer,[30] list entropies for the aqueous tripositive ions of Al, Fe, and Gd. A plot of these values vs. ionic radii yields an essentially straight line from which one obtains $S^{\circ}_{Eu^{+3}} = -43.0$ e.u. for $r_{Eu^{+3}} = 1.03$Å.[31] A similar plot of the dipositive ions yields $S^{\circ}_{Eu^{+2}} = -6.7$ e.u. for $r_{Eu^{+2}} = 1.12$Å[31].

The equations involved are:

$$Eu + 2H^{+}_{(aq)} \longrightarrow Eu^{+2}_{(aq)} + H_2 \qquad (2)$$

$$Eu^{+2}_{(aq)} + H^{+}_{(aq)} \longrightarrow Eu^{+3}_{(aq)} + \tfrac{1}{2}H_2 \qquad (11)$$

The sum of these two reactions is just the reaction for the formation of $Eu^{+3}_{(aq)}$ from the metal and hydrogen ion for which $\Delta H^{\circ} = -130.4$ Kcal/mole. The enthalpy change for (11) is:

$$\Delta H^{\circ} = \Delta F^{\circ} + T\Delta S^{\circ}$$

$$= -n\mathcal{F}\mathcal{E}' + T\Delta S^{\circ}$$

$$= -1 \times 23{,}060 \times 0.43 + 298(-43.0 + 15.6 + 6.7)$$

$$= -16.1 \text{ Kcal/mole}$$

ΔH° for reaction (2) is then - 130.4 + 16.1 or - 114.3 Kcal/mole which is the heat of formation of $Eu^{+2}_{(aq)}$.

The Eu - Eu^{+2} aqueous potential can be calculated from the heat of formation of $Eu^{+2}_{(aq)}$ and the entropy of europium metal. Habermann and Daane[32] estimate S°_{Eu} = 19.3 e.u. From this we calculate

$$\Delta F = \Delta H - T\Delta S$$

$$= - 114.3 - 298(- 6.7 + 31.2 - 19.3)$$

$$= - 115.8 \text{ Kcal.}$$

$$\varepsilon^\circ = \frac{- 115.8}{- 2 \times 23.1}$$

$$= 2.51 \text{ v.}$$

Shul'gin[28] gives an expression for the dependence of the equlibrium constant for (11) on temperature from which ΔS can be calculated:

$$\ln K_{eq} = \left(\frac{7.197}{T}\right) - 7.44$$

$$\Delta F = - RT\left(\frac{7.197}{T} - 7.44\right)$$

$$= - 14.3 + 14.8T$$

$$\Delta S = - \left(\frac{\partial \Delta F}{\partial T}\right)_P = - 14.8 \text{ e.u.}$$

From this one calculates ΔH for (11) to be - 14.3 Kcal and $\Delta H^\circ_{fEu^{+2}}$ = - - 116.1 Kcal. The Eu - Eu^{+2} aqueous potential is then 2.57 v. These are in reasonable agreement with our values.

Since there is much more data available for the entropies of the dipositive aqueous ions than the tripositive, the Brewer plot is likely to give a better value for the entropy of $Eu^{+2}_{(aq)}$ than $Eu^{+3}_{(aq)}$. Therefore using $S^\circ_{Eu^{+2}}$ = - 6.7 e.u. from the Brewer plot, and the ΔS for reaction (11) of - 14.8 e.u. calculated from Shul'gin's expression, we calculate $S^\circ_{Eu^{+3}_{(aq)}}$ = - 37.1 e.u.

It is the opinion of the author that a more accurate value for $S^\circ_{Eu^{+3}_{(aq)}}$ could be calculated from heats of solution data on $EuCl_{2(c)}$, as was indicated previously, and the present estimate for $S^\circ_{Eu^{+2}_{(aq)}}$.

With the heat of solution of $EuO_{1.021}$ (or $EuO{\cdot}0.021Eu_2O_3$) in 1N HCl, the previously determined heat of formation of $Eu^{+3}_{(aq)}$, and the heat of formation of Eu_2O_3, we can calculate the heat of formation of $EuO{\cdot}0.021Eu_2O_3$ using equation (7). The correction to the infinitely dilute standard state can be approximated from the data of Westrum and Robinson[33] on the heat of solution of $PuCl_{3(c)}$ in different concentrations of hydrochloric acid. An extrapolation of their data gives a difference of - 1.5 Kcal between 1.00M HCl and infinate dilution. Thus:

$$\Delta H^{o}_{fEuO{\cdot}0.021Eu_2O_3} = 1.042\,\Delta H_{fEu^{+3}_{(aq)}} + 1.563\,\Delta H_{fH_2O} - \Delta H_{soln}$$

$$= - 135.9 - 106.8 + 89.3$$

$$= - 153.4 \pm 2.0 \text{ Kcal/mole}$$

There is available one value for comparison with this number. The heat of combustion of $EuO_{1.02}$ to Eu_2O_3 was done on a small sample and the rough value of 350 cal/g obtained.[34] From this and the value for the standard heat of formation of Eu_2O_3[35], we calculate

$$\Delta H^{o}_{fEuO_{1.02}} = - 136 \text{ Kcal/mole.}$$

The difference between these two values is large, but the sample for the combustion experiment was far too small for an accurate measurement and the resulting uncertainty is likely to be appreciable.

The heat of formation of pure $EuO_{(c)}$ is then the heat of formation of $EuO{\cdot}0.021\ Eu_2O_3$ minus 0.021 times the heat of formation of Eu_2O_3. We calculate:

$$\Delta H^{o}_{fEuO_{(c)}} = - 153.4 + 0.021 \times 393.9$$

$$= - 145.1 \pm 2.2 \text{ Kcal/mole.}$$

For comparison, the standard heats of formation of other monoxides[15,23] are given in Table XI. Considering the heats of formation, EuO is quite unlike the transition metal monoxides and very much like the alkaline earth monoxides. But, on the other hand, "EuO", as prepared, is non-stoichiometric like the transition metal "monoxides".

TABLE XI

Thermodynamic Properties
of Some Monoxides

	ΔH_f°	S°		ΔH_f°	S°		ΔH_f°	S°
MgO	- 143.8	6.4	MnO	- 92.0	14.4	BiO	- 49.9	(17)
CaO	- 151.9	9.5	$Fe_{0.95}O$	- 63.7	12.9	GeO	- 73	(12)
SrO	- 141.1	13.0	CoO	- 55.2	10.5	PbO	- 52.4	16.2
BaO	- 133.4	16.8	CuO	- 37.1	10.4	SnO	- 68.4	13.5
EuO	- 145.1	(16.3)	NiO	- 58.4	9.2	HgO	- 21.7	17.2
			ZnO	- 83.2	10.5	RhO	- 21.7	(13)
			CdO	- 60.9	13.1	PdO	- 20.4	(13)

Concerning the stability of EuO, we can consider the disproportionation reaction:

$$3EuO \longrightarrow Eu + Eu_2O_3$$

$$\Delta H_D = \Delta H^\circ_{fEu_2O_3} - 3\,\Delta H^\circ_{fEuO}$$

$$= -393.9 + 435.3$$

$$= +41.4 \text{ Kcal/mole}$$

The change in entropy, ΔS°_D, can be calculated from available estimates: (36,32)

$$\Delta S^\circ_D = S^\circ_{Eu_2O_3} + S^\circ_{Eu} - 3S^\circ_{EuO}$$

$$= 35 + 19 - 3 \times 16.3$$

$$= 5 \text{ e.u.}$$

From these two values the change in the Gibbs free energy and the disproportionation constant, K_D, can be calculated:

$$\Delta F_D = \Delta H_D - T\Delta S_D$$

$$= 41{,}400 - 298 \times 5$$

$$= 39{,}910 \text{ cal.}$$

$$\Delta F_D = -RT \ln K_D$$

$$\ln K_D = -\frac{39{,}910}{1.987 \times 298}$$

$$= -67.42$$

$$K_D = 5.3 \times 10^{-30}$$

This indicates considerable stability to disproportionation at 25°C. Preparation temperatures known to this author have ranged from about 1250°C to about 1650°C, so the equlibrium is shifted far to the "monoxide" side, and we see that EuO has considerable stability over a wide range of temperature.

Because of its electronic configuration- $(Xe)4f^7 5d^0 6s^2$ - europium metal is dipositive and hence very different from most of the other rare earth metals. Since the metals are the reference states for thermo-

chemical measurements, this difference is reflected in the values for the thermodynamic properties of corresponding species.

Again because of its electronic configuration europium forms relatively stable dipositive species in which it closly resembles the alkaline earths. This is presently seen in the thermodynamic properties of the dipositive aqueous ion and the monoxide.

Europium "monoxide" is also seen to resemble the transition metal "monoxides" in that it is non-stoichiometric. The present paper indicates that the oxygen - to-- europium ratio is greater than one.

Further work along this line should include similar studies on ytterbium, as it is like europium in several ways, and also samarium and thulium since the dipositive valence state has been observed there also.

Acknowledgments

The author expresses his sincere thanks to Professor Burris B. Cunningham, whose guidance and suggestions always helped in the solution of the problem.

A special word of thanks is due Dr. James C. Wallmann for his helpful assistance and suggestions; Mr. Herman P. Robinson for his expert help in maintaining and improving the calorimeter; Mr. George Shalimoff for doing the many spectrographic analyses; and of first importance, my wife who provided much needed moral support.

My thanks to Mr. Tom Parsons for his aids in experimental technique; to Messrs. Bert Watkins, Hap Hagopian, Billy Abram, and Harry Powell for their expert help in constructing the apparatus used; and to Mr. Jere Green, Dr. Moshè Zirin, Mr. Sayed Marei, and Dr. Jean Fuger for their assistance and our helpful discussions.

The help of Miss Lilly Goda, Mrs. Lillian White, and Mrs. Gertrude Bolz for laboratory assistance is appreciated.

This work was done under the auspices of the United States Atomic Energy Commission.

References

1. S. R. Gunn, Thermodynamics of the Aqueous Ions of Americium, UCRL - 2541, (Ph.D. Thesis), April, 1954.
2. C. H. Shomate and E. H. Huffman, J. Am. Chem. Soc. 65, 1625 (1943).
3. A.Glasner, E. Levy, and M. Steinberg, J. I. N. C. 25, 1415 (1963).
4. B. D. Abram, T. C. Parsons, and P. W. Howe, UCRL - 10367, 1962.
5. J. C. Achard, Compt. Rend. 250, 3025 (1960).
6. Von H. Baernighausen and G. Brauer, Acta. Cryst. 15, 1059 (1962).
7. H. A. Eick, N. C. Baenziger, and L. Eyring, J. Am. Chem. Soc. 78, 5147 (1956).
8. B. T. Matthias, R. M. Bozorth, and J. H. Van Vleck, Phys. Rev. Letters 7, 160 (1961).
9. J. C. Warf and W. L. Korst, N. P. - 6078 (June 1956).
10. F. H. Ellinger, C. C. Land, and E. M. Cramer, Extractive and Physical Metallurgy of Plutonium and its Alloys, W. D. Wilkinson, Ed. (Interscience Publishers, Inc., New York, 1960).
11. F. H. Ellinger, AECU - 2593 (1953).
12. A. F. Wells, Structural Inorganic Chemistry, 3rd Ed. (Oxford University, Clarendon Press, London, 1962).
13. D. M. Smyth, Phys. and Chem. of Solids 19, 167 (1961).
14. C. T. Stubblefield and L. Eyring, J. Am. Chem. Soc. 77, 3004 (1955).
15. Selected Values of Chemical Thermodynamic Properties, U. S. Bureau of Standards Circular 500 (Washington D. C., 1952).
16. F. Spedding and J. Flynn, J. Am. Chem. Soc. 76, 1474 (1954).
17. F. Spedding and C. Miller, J. Am. Chem. Soc. 74, 4195 (1952).
18. R. L. Montgomery, U. S. B. M. R. I. 5525 (1959).
19. K. A. Geschneidner Rare Earth Alloys, (D. Van Nostrand Co., Inc., 1961).

20. F. H. Spedding and G. Atkinson, Properties of Rare Earth Salts in Electrolytic Solutions, in The Structure of Electrolytic Solutions, edited by Walter J. Hamer (John Wiley & Sons, Inc., New York, 1959).

21. J. P. Surls and G. R. Choppin, J. Am. Chem. Soc. 79, 855 (1957).

22. Chr. Klixbüll Jørgensen, Orbitals in Atoms and Molecules (Academic Press, 1962).

23. W. Latimer, Oxidation Potentials, 2nd Ed. (Prentice - Hall, 1952).

24. H. Bommer and E. Hohmann, Z. an. u. allg. Ch. 248, 357 (1941).

25. H. McCoy, J. Am. Chem. Soc. 58, 1578 (1936).

26. W. Noddack and A. Brukl, Angew. Chem. 50, 362 (1937).

27. H. Laitinen and W. Taebel, Ind. and Eng. Chem. 13, 825 (1941).

28. L. P. Shul'gin and Yu. A. Koz'min, Zh. Fiz. Khim. 37 (8), 1857 (1963).

29. L. Brewer, et. al., Chemistry and Metallurgy of Miscellaneous Materials. Thermodynamics, National Nuclear Energy Series IV - 19B Paper 6 (McGraw - Hill Book Co. 1949).

30. G. N. Lewis and M. Randall, Thermodynamics, 2nd Ed. rev. by K. Pitzer and L. Brewer (McGraw - Hill Book Co., New York, 1961).

31. L. Pauling, The Nature of the Chemical Bond, 3rd Ed. (Cornell University Press, 1960).

32. C. E. Habermann and A. H. Daane, J. Chem. Phys. 41, 2818 (1964).

33. E. F. Westrum, Jr. and H. P. Robinson, The Transuranium Elements, National Nuclear Energy Series IV - 14B Paper 6.54 (McGraw - Hill Book Co., 1949).

34. Charles E. Holley, Jr. (LosAlamos Scientific Laboratory, Los Alamos, New Mexico), private communication, June, 1963.

35. Charles E. Holley, Jr. (Los Alamos Scientific Laboratory, Los Alamos, New Mexico), private communication, January, 1964.

36. E. F. Westrum, Jr. and F. Grønvold, Chemical Thermodynamics of the Actinide Element Chalcogenides, Paper SM - 26/30, presented at the International Atomic Energy Agency Symposium on Thermodynamics of Nuclear Materials, Vienna, 1962.